SF2A 2012
S. Boissier, P. de Laverny, N. Nardetto, R. Samadi, D. Valls-Gabaud and H. Wozniak (eds)

PULSATIONS-CONVECTION COMBINATION IN STARS

S. Félix[1], E. Audit[1] and B. Dintrans[2]

Abstract. The κ-mechanism and the Cepheids' instability band have been studied and modeled in 1D and 2D cartesian boxes with the Pencil code (Thomas Gastine's thesis work and papers). We intend to extend this work to 3D simulations with the hydrodynamic code Heracles. First step is getting hydrostatic equilibrium with sufficient precision so that future added features will be correctly performed. 1D and 2D cases are explored, both with isothermal and ideal gas evolutions with Heracles. Those equilibria are then perturbated by an overdensity. First results show that we manage to get a fairly good equilibrium profile with negligible residual velocities.

Keywords: hydrostatic equilibrium, simulations, Heracles, Cepheid, κ-mechanism

1 Introduction

Cepheids are variable stars from the instability strip of the Hertzsprung-Russel diagram. They have a variable luminosity (and radius) linked to the famous period-luminosity relationship used to calculate star's distances. These periodic variations were explained by Eddington (1917) through the κ-mechanism, an excitation mechanism of stellar oscillations that is related to the opacity in ionisation regions.

The blue edge of the classical instability strip (where stars have higher surface temperature) is rather well-known and explained (Chiosi et al. (1993); Beaulieu et al. (1995)) but cold Cepheids close to the red edge present a convective zone at their surface that affects their pulsation properties.

These cold Cepheids were poorly described by complex models with a large number of unconstrained (if not degenerate) free parameters (Yecko et al. (1998); Buchler (2009); Gastine & Dintrans (2011a)), until Thomas Gastine performed 1D and 2D direct numerical simulations that correctly took into account the nonlinearities involved in the convection-pulsation coupling (Gastine & Dintrans (2011b)), using the Pencil Code.

Among other things, he showed that, for a given position in the layer, the hollow amplitude and width of the conduction profile stand out as the key parameters governing the occurrence of unstable modes driven by the κ-mechanism (Gastine & Dintrans (2008)).

These authors then studied the physical conditions needed to lead to a quenching of oscillations by convection. Indeed, in cold Cepheids, a coupling occurs between the acoustic oscillations and the convective motions close to the surface: hence, the surface convective zone stabilises the radial oscillations excited by the κ-mechanism. It was shown that a larger stratification in density leads to smaller convective plumes that do not affect the purely radial modes much, while large-scale vortices may quench the oscillations.

But the convection is an intrinsically 3D phenomenon so it is necessary to get to know what happens in 3D simulations. In order to do that, we are using the Heracles hydrodynamic simulation code from CEA, France. The first step is to reproduce Thomas Gastine's results obtained in 1D and 2D with this code and, first of all, constructing 1D and 2D hydrostatic equilibrium for isothermal or ideal gas.

First results are shown here, for isothermal and ideal gas, first for 1D and then for 2D equilibrium.

2 Hydrostatic equilibrium with Heracles

Heracles is a 3D hydrodynamical code used to simulate astrophysical fluid flows. It uses a finite volume Godunov method on a fixed grid to solve, in our first simple study case, the equations of hydrodynamics and gravity. We are using a 1D or 2D cartesian grid of physical size $l \times L$.

[1] CEA - Maison de la Simulation (USR3441), Gif-sur-Yvette, France.
[2] IRAP, CNRS/Université de Toulouse (UMR5277), 14 av. Edouard Belin, F-31400 Toulouse, France

2.1 1D equilibrium

We ran first isothermal ($\gamma = 1$) then ideal gas ($\gamma = \frac{5}{3}$) 1D simulations, using a 1D "box" $l = 1$, divided in a grid of constant spacing Δx.

Initial conditions are taken so as to reproduce hydrostatic equilibrium with a uniformed temperature: density is the usual theoretical integrated exponential profile

$$\rho_i = \frac{1}{\Delta x}\int_{x_i}^{x_{i+1}} \rho_0 \exp(-x/h)\mathrm{d}x = \rho_0 \frac{h}{\Delta x}\left[\exp(\Delta x/h) - 1\right]\exp(-i\Delta x/h), \tag{2.1}$$

so that ρ_i is the mean value of ρ over the grid cell i located at $x_i = (i-1)\Delta x$. Sound speed is $c_s = 1$ and gravity is $|g| = 1/2$, constant and directed along the x axis, towards negative values. Hence, the pressure height is $h = c_s^2/(\gamma|g|) = 2$. Finally, 1D fluid velocity is null everywhere, so that energy is only $E = P/(\gamma - 1)$ where P is the gas pressure.

The important part is boundary conditions. We have two fictive zones at each side of the domain. Hydrostatic equilibrium at constant temperature is prolonged for density and energy at each side of the domain and reflexive velocity conditions are imposed (i.e. mass flux is null at the external interfaces). Finally we are also using logarithm slopes for density and energy calculations, to get more precise results.

We obtain the following results first for an isothermal equation of state (left column of Figure 1) and then for an ideal gas (right column). In both cases, density profiles (upper panels are theoretical and simulated density profiles and middle panels are the difference between those two densities) are quite satisfying. Velocities (lower panels) should be exactly zero, as we reached hydrostatic equilibrium. Nevertheless, some residual velocities might appear due to inevitable computational approximations (rounding errors...) but are quite small (at most 10^{-6} smaller than the sound speed, that is way smaller than the fluctuations we will later be interested in) and thus negligeable.

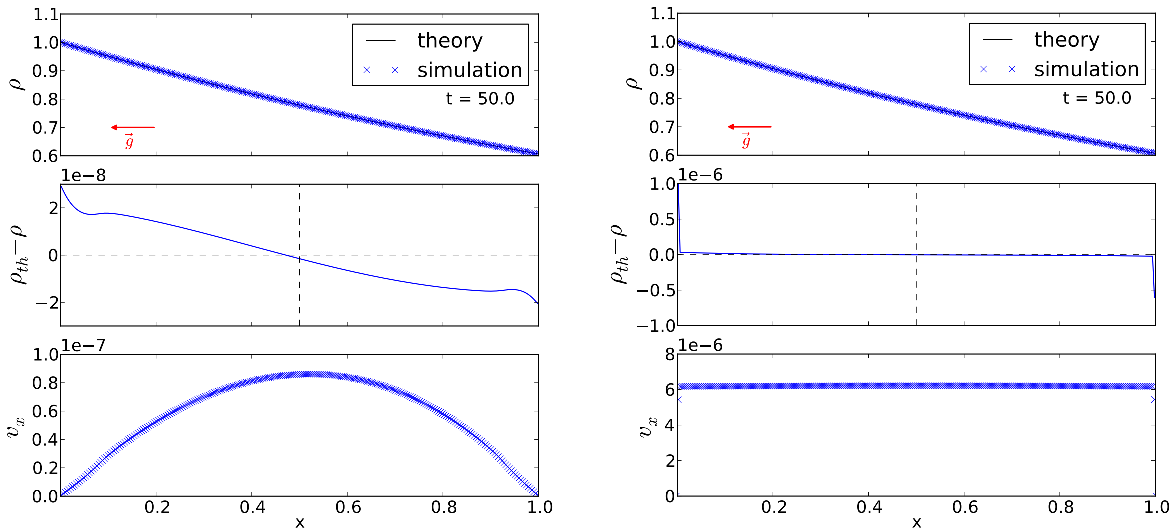

Fig. 1. Results of Heracles code for an isothermal (**Left column**) and ideal gas (**Right column**) 1D hydrostatic equilibrium at final time $t = 50.0$. **Upper panels:** simulated and theoretical densities $\rho(x)$. **Middle panels:** difference between theoretical and simulated densities $\rho_{th} - \rho$. **Lower panels:** velocity profiles along x-axis. The arrow $\vec{g}$ indicates the used gravity vector.

When a perturbation is added to the previous (isothermal or adiabatic) equilibrium, such as a smooth overdensity (later referenced to as a "density bubble", Figure 2), acoustic oscillations in density profile are expected until the fluid reaches equilibrium, after a characteristic time of $\tau_{\rm dyn} \sim 1/\sqrt{G < \rho >}$ where $< \rho >$ is the mean density value (e.g. Dintrans & Brandenburg 2004). This is obviously a new equilibrium since the box contains more mass now: the red line in Figure 2 is above the initial blue line. From these oscillations, a characteristic Fourier decomposition of the velocity is computed and results are given in Figure 3 upper panel for the isothermal case. The frequencies of these oscillations can be computed analytically and this figure shows that our simulations are in good agreement with theoretical values $\omega_n = c_s\sqrt{k_z^2 + 0.25/h^2}$, with $k_z = (n+1)\pi$ and n the radial order of the acoustic mode.

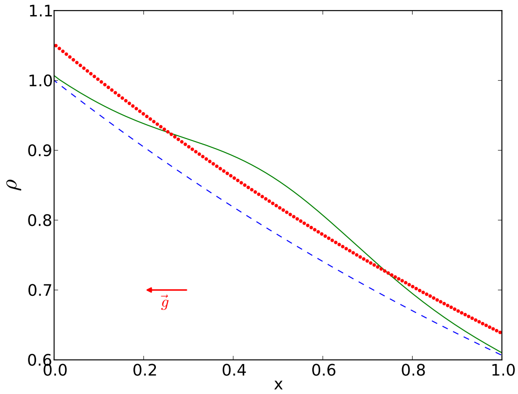

Fig. 2. Results of Heracles code for an isothermal 1D hydrostatic equilibrium perturbated by a density bubble: the dashed blue line is the density profile at equilibrium before the addition of the bubble ; the continuous green line is the density profile at the timestep when the bubble is added and the dotted red line shows the density profile at the end of the simulation when a new equilibrium has been reached. The arrow $\vec{g}$ indicates the used gravity vector.

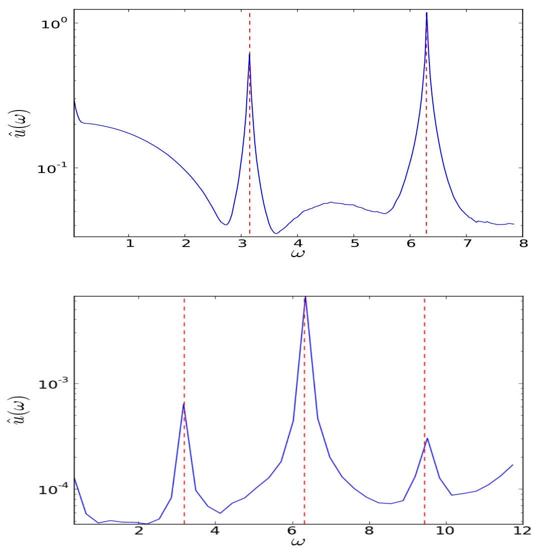

Fig. 3. Fourier spectra obtained for the 1D (**Upper panel**) and 2D (**Lower panel**) isothermal case with a bubble: theoretical frequencies are shown in red dashed lines.

2.2 2D equilibrium

In this case, we perform 2D isothermal and ideal gas simulations with the same options as in 1D simulations, except the following 2D features:

- Parameters: 2D box with $l = 1$, $L = 1$, divided in a grid of constant spacing $\Delta x \times \Delta y$.
- Initial conditions: on the x-axis, we get the same exponential profile for all the points of the y-axis.
- Boundary conditions: on the y-axis, boundary conditions are periodic.

The hydrostatic equilibrium is stable in both cases and, as in 1D equilibrium, residual velocities are negligeable. Figure 4 upper row shows an unperturbated isothermal 2D hydrostatic equilibrium: we can see that 2D equilibrium behaves like a juxtaposition of 1D equilibria.

When a density perturbation is added to the previous equilibrium (Figure 4 middle row), oscillations develop until the fluid reaches equilibrium again (again, it is a new equilibrium with more mass, as shown in Figure 4 lower row). The Fourier decomposition is also in good agreement with theoretical frequencies, as the lower panel in Figure 3 shows.

3 Conclusions

With HERACLES, we obtain a fairly good hydrostatic equilibrium with very small residual velocities. Theoretical frequencies are found if the equilibrium is perturbated by a density bubble and a new equilibrium is reached after some time. This will be quite important since we are going to implement complex conduction profiles and instabilities. We aim at extending these studies to a 3D cartesian box with HERACLES.

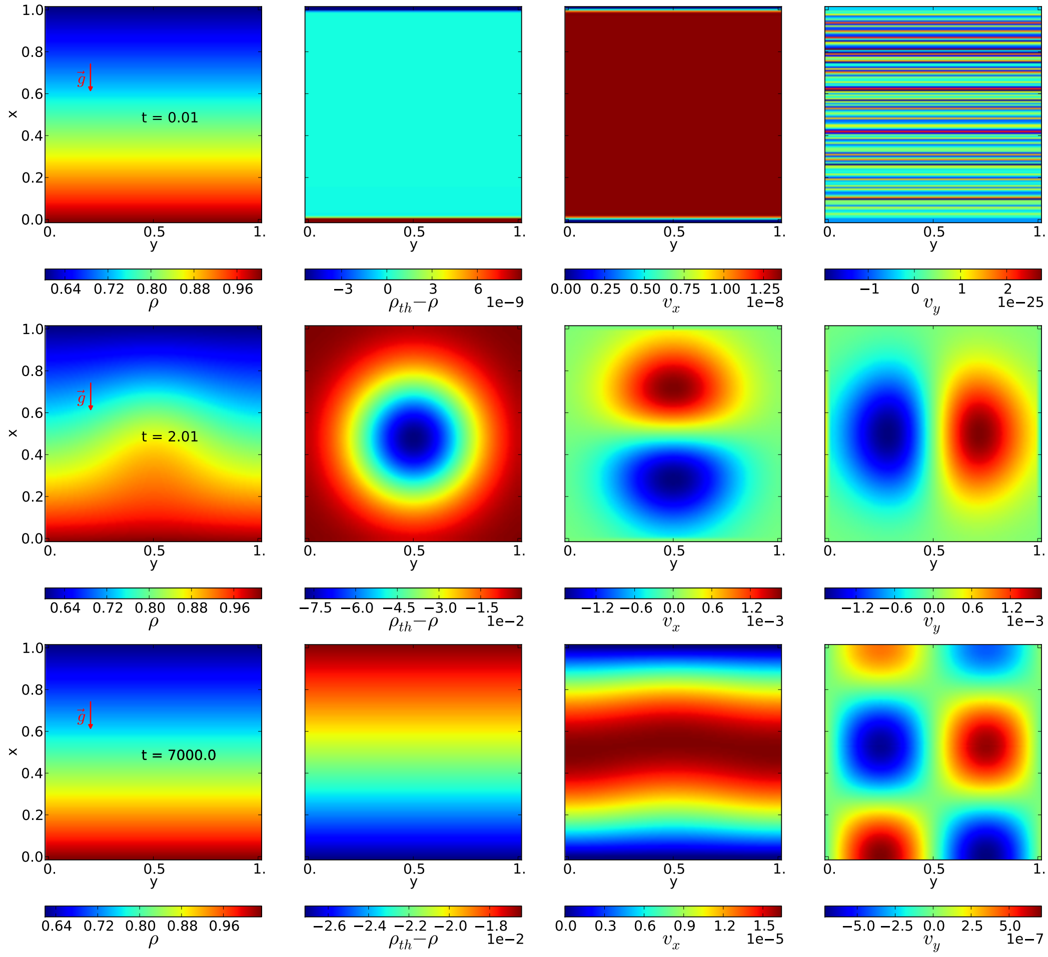

Fig. 4. Results of Heracles code for an isothermal 2D hydrostatic equilibrium before a bubble is added (**Upper row**, time 0.01), at the timestep the bubble is added (**Middle row**, time 2.0) and when the new equilibrium is reached (**Lower row**, final time 7000). **From left to right, first column:** density profile $\rho(x, y)$; **second column:** difference between theoretical (without perturbation) and simulated densities $\rho_{th} - \rho$; **third column:** velocity profile along x-axis $v_x(x, y)$; **fourth column:** velocity profile along y-axis $v_y(x, y)$. The arrow $\vec{g}$ indicates the used gravity vector.

References

Beaulieu, J. P., Grison, P., Tobin, W., et al. 1995, A&A, 303, 137

Buchler, J. R. 2009, in American Institute of Physics Conference Series, Vol. 1170, American Institute of Physics Conference Series, ed. J. A. Guzik & P. A. Bradley, 51–58

Chiosi, C., Wood, P. R., & Capitanio, N. 1993, ApJS, 86, 541

Dintrans, B. & Brandenburg, A. 2004, A&A, 421, 775

Eddington, A. S. 1917, The Observatory, 40, 290

Gastine, T. & Dintrans, B. 2008, in SF2A-2008: Proceedings of the Annual meeting of the French Society of Astronomy and Astrophysics, ed. C. Charbonnel, F. Combes, & R. Samadi, 471–474

Gastine, T. & Dintrans, B. 2011a, A&A, 530, L7

Gastine, T. & Dintrans, B. 2011b, in SF2A-2011: Proceedings of the Annual meeting of the French Society of Astronomy and Astrophysics, ed. G. Alecian, K. Belkacem, R. Samadi, & D. Valls-Gabaud, 215–219

Yecko, P. A., Kollath, Z., & Buchler, J. R. 1998, A&A, 336, 553